

1

2 Microscopic driving theory with non-hypothetical congested steady 3 state: Model and Empirical verification

4

5 Jun-fang Tian*, Zhen-zhou Yuan, Bin Jia, Wen-yi Zhang

6 *MOE Key Laboratory for Urban Transportation Complex Systems Theory and Technology, Beijing Jiaotong*
7 *University, Beijing, 100044, China*

8

9 The essential distinction between the fundamental diagram approach and three-phase theory is the
10 existence of unique space-gap-speed relationship. In order to verify this relationship, empirical
11 data are analyzed with the following findings: (1) linear relationship between the actual space gap
12 and speed can be identified when the speed difference between vehicles approximate zero; (2)
13 vehicles accelerate or decelerate around the desired space gap most of the time. To explain these
14 phenomena, an assumption and a new cellular model are proposed that in the noiseless limit
15 vehicles' space gap will fluctuate around the desired space gap, rather than keep the desired space
16 gap, in the homogeneous congested traffic flow. Then, simulations under periodic and open
17 boundary conditions are carried out. Results show that empirical findings of three-phase theory
18 can be well reproduced. Finally, Model is calibrated and validated. All validation results are
19 acceptable and better than previous studies.

20 **Key words:** cellular automaton; three-phase traffic flow; fundamental diagram; safe time gap;

21

22 1. Introduction

23 With the rapid development of urbanization, traffic congestion becomes one of the most serious problems that
24 undermine the operation efficiency of modern cities. In order to understand the mechanism of traffic congestion, many
25 models and analysis have been carried out to explain the empirical findings (see the reviews: Haight, 1963; Whitham,
26 1974; Leutzbach, 1987; Treiber and Kesting, 2013; Chowdhury, 2000; Helbing, 2001; Nagatani, 2002; Jia et.al. 2007;
27 Kerner, 2004, 2009;) Generally speaking, these models can be classified into the fundamental diagram approach and
28 the three-phase theory, which are the main branches of the traffic flow theories.

29 Originated from Greenshields (1935), the fundamental diagram permeates in all levels of traffic flow models and
30 is one of the basic research technics of empirical data. Fundamental diagram is the idealized form of the flow-density
31 curve in traffic flow, which goes through the origin with at least one maximum. It describes the theoretical relation
32 between density and flow in stationary homogeneous traffic, i.e., the steady state equilibrium of identical
33 driver-vehicle units (Treiber and Kesting, 2013). In the last century, almost all traffic flow models belong to the
34 fundamental diagram approach. In microscopic models, the fundamental diagram is linked to the steady-state of
35 car-following (CF) or Cellular automata (CA) models. For example, in the Optimal Velocity Model (OV model), the
36 fundamental diagram exits in the optimal velocity function (Bando et.al., 1995); In the Nagel-Schreckenberg cellular

* Corresponding author.

E-mail address: tianhustbjtu@hotmail.com

1 automaton model (NaSch model), it could be derived in the steady states (Nagel and Schreckenberg, 1992). In
2 macroscopic or mesoscopic models, it has been directly applied (e.g. the LWR theory (Lighthill and Whitham, 1955;
3 Richards, 1956)) or incorporated into the momentum equation (e.g. the PW theory (Payne, 1979)). Generally speaking,
4 models within the fundamental diagram approach have a fundamental diagram of steady states in the unperturbed,
5 noiseless limit cases (Kerner, 2004, 2009).

6 The majority of models in fundamental diagram approach belong to the two-phase models (Lighthill and
7 Whitham, 1955; Payne 1979; Richards, 1956; Herman et. al., 1959; Tang 2005; Newell, 2002; Gipps, 1981; Bando
8 et.al., 1995; Treiber et.al., 2000; Nagel and Schreckenberg, 1992), which refers to the free flow phase (F) and the
9 jammed phase (J). The phase transitions involved is the transition from free flow to jams (F→J transition) and the
10 transition from jam to free flow (J→F transition). Two mainly different explanations of the jam formation are given in
11 the fundamental diagram approach. The first is the instability of traffic flow, which is closely related with the finite
12 reaction time of drivers. When the leading driver begins to decelerate, the following driver will decelerate stronger
13 than the leading after some finite time to avoid accidents (e.g. GM car following model (Herman et. al., 1959)). The
14 second is the existence of the metastable free flow in some density region. If the amplitude of a local perturbation
15 exceeds some critical amplitude, the perturbation will grow and lead to jams (e.g. PW model (Payne, 1979)).

16 Based on long-term empirical analysis, Kerner (2004, 2009) believes that two-phase models could not reproduce
17 the features of traffic breakdown as well as the further development of the related congested region properly. Then
18 they introduced the three-phase theory, in which there are (1) free traffic flow (2) synchronized flow and (3) wide
19 moving jams. The fundamental hypothesis of the three-phase theory is that the hypothetical steady states of the
20 synchronized flow cover a two-dimensional region in the flow-density plane, in other words there is no fundamental
21 diagram of traffic flow. Over the time, there are many traffic flow models within the framework of three-phase theory
22 (Kerner et.al., 2002, 2011; Kerner, 2012; Kerner and Klenov 2002, 2003, 2006; Lee et.al., 2004; Jiang and Wu, 2003,
23 2005; Tian et.al., 2009; Gao et.al., 2007, 2009; Davis, 2004). In order to improve readability, we have made a brief
24 introduction of the three-phase theory and its models needed for understanding the paper in the appendix.

25 It should be noted that there are three-phase models in the framework of the fundamental diagram approach, such
26 as the break light cellular automaton model (BLM (Knospe, 2000)), the speed adaption three-phase traffic models
27 (SAMs (Kerner and Klenov, 2006)), and the average space gap cellular automaton model (ASGM (Tian et al.,
28 2012a,2012b)). However, some of these models have been criticized by the three-phase theory. BLM has been
29 criticized because its congested patterns are inconsistent with the empirical findings (Kerner et.al., 2002). SAMs are
30 not able to reproduce the local synchronized patterns (LSPs) consistent with empirical results as well as some of
31 empirical features of synchronized flow between wide moving jams within general patterns (GPs) (Kerner and Klenov,
32 2006). But these critics cannot apply to ASGM, which can describe the LSPs and GPs very well.

33 Although this paper originates from the inconsistency research between fundamental diagram approach and
34 three-phase theory, the purpose is not to discuss their controversies. This paper aims to describe the driver behaviors
35 by a cellular automaton model based on the empirical observation, which can describe the three-phase theory very
36 well. Empirical validations show higher accuracy than precious studies. To these ends, section 2 analyses the US-101
37 trajectory datasets on a single freeway lane, away from lane changes and bottleneck influence. In order to explain the
38 empirical observations, an assumption is proposed, i.e., in the noiseless limit, vehicles' space gap will fluctuate around
39 the desired space gap, rather than keep the desired space gap, in the homogeneous congested traffic flow. Section 3
40 proposes a cellular model that incorporates this assumption. Empirical findings of three-phase theory are simulated
41 and discussed in section 4. Furthermore, section 5 has calibrated and validated the model with the I-80 detector data.
42 Finally, the conclusion is given in section 6.

44 2. Empirical data analysis

45 The essential distinction between the fundamental diagram approach and the three-phase theory is whether the

fundamental diagram exists. Three-phase theory supposes the existence of a two-dimensional region of hypothetical homogenous synchronized flow in the space-gap-speed plane. Drivers can make an arbitrary choice in the space gap within a certain region. The fundamental diagram approach assumes the existence of a space-gap speed relationship. For example, the IDM model presumes the following relationship (Treiber and Kesting, 2013):

$$s^*(v, \Delta v) = s_0 + vT + \frac{v\Delta v}{2\sqrt{ab}} \quad (1)$$

where s^* is the desired gap. The meanings and typical values of IDM are shown in Tab. 1. The relationship between space gap s and speed v in the steady state is $s = s_0 + vT$, which also permeates in other car following models, such as Newell's model (Newell, 2002). Thus, the validation of $s = s_0 + vT$ contributes to resolve these controversies between the fundamental diagram approach and three-phase theory. However, it is impossible to validate this relationship by the real traffic directly, since real traffic flow is always in the non-equilibrium state, i.e., the desired gap is hardly to be achieved. Nevertheless, Equation (1) indicates that we can validate the equation $s = s_0 + vT$, if the velocity between vehicles approximate zero. In order to exclude the influence of the velocity difference Δv , we only analysis the empirical data with $\Delta v \leq \Delta v_c$. The value of Δv_c should be able to neglect the influence of Δv and meanwhile make the empirical sample size large enough. Δv_c is determined by the analysis of equation (1). Assuming if $\Delta v \leq \Delta v_c$, then $s^* \approx s_0 + vT$. For the typical value given in Tab. 1, $s^* \approx 2 + 1.5v + 0.3v\Delta v$. Thus, if $1.5v \gg 0.3v\Delta v_c$, i.e. $1.5 \gg 0.3\Delta v_c$, then $s^* \approx s_0 + 1.5v$. A suitable value for Δv_c is $0.1m/s$

Table 1
Model Parameters and values of IDM (Treiber and Kesting, 2013)

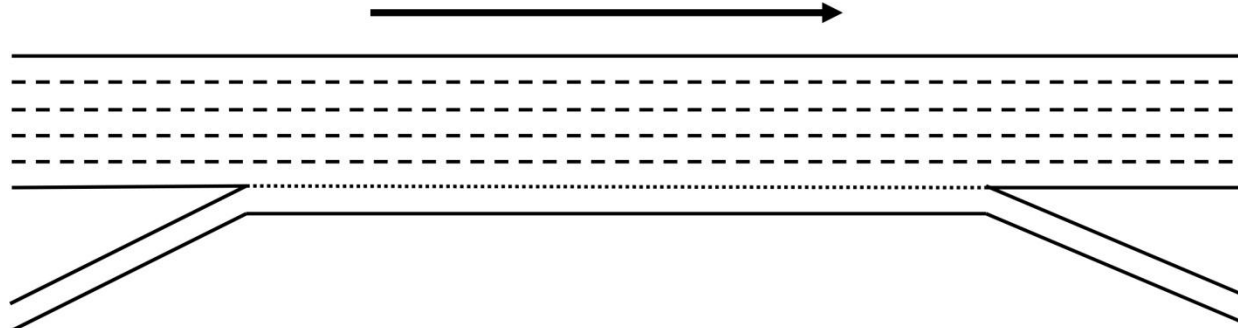
Parameter (units)	Typical value	Reasonable range
Time gap $T(s)$	1.5	0.9~3
Minimum gap $s_0(m)$	2	1~5
Acceleration $a(m/s^2)$	1.4	0.3~3
Comfortable deceleration $b(m/s^2)$	2.0	0.5~3

Next, the US-101 trajectory datasets of the Next Generation Simulation Community (NGSIM, 2006) are applied to validate $s = s_0 + vT$. These data were collected on a $640m$ segment on the south-bound direction of US 101 (Hollywood Freeway) in Los Angeles, California on June 15th, 2005. The data were detected from 7:50 a.m. to 8:05 a.m., 8:05 a.m. to 8:20 a.m., and 8:20 a.m. to 8:35 a.m. During the data collection period, the California Highway Patrol's Computer Aided Dispatch (CHP CAD) system was monitored. No traffic incidents were recorded during the morning of June 15th on US 101 within the study area or on any upstream/downstream sections likely influencing traffic in the study area. Fig.1 provides a schematic illustration of the location for the vehicle trajectory datasets. There are five mainline lines throughout the section, and an auxiliary lane is present through a portion of the corridor between the on-ramp and off-ramp. In order to minimize the impact of bottleneck on traffic flow, only the leftmost lane is analyzed. The following criteria are used to pick up the empirical data:

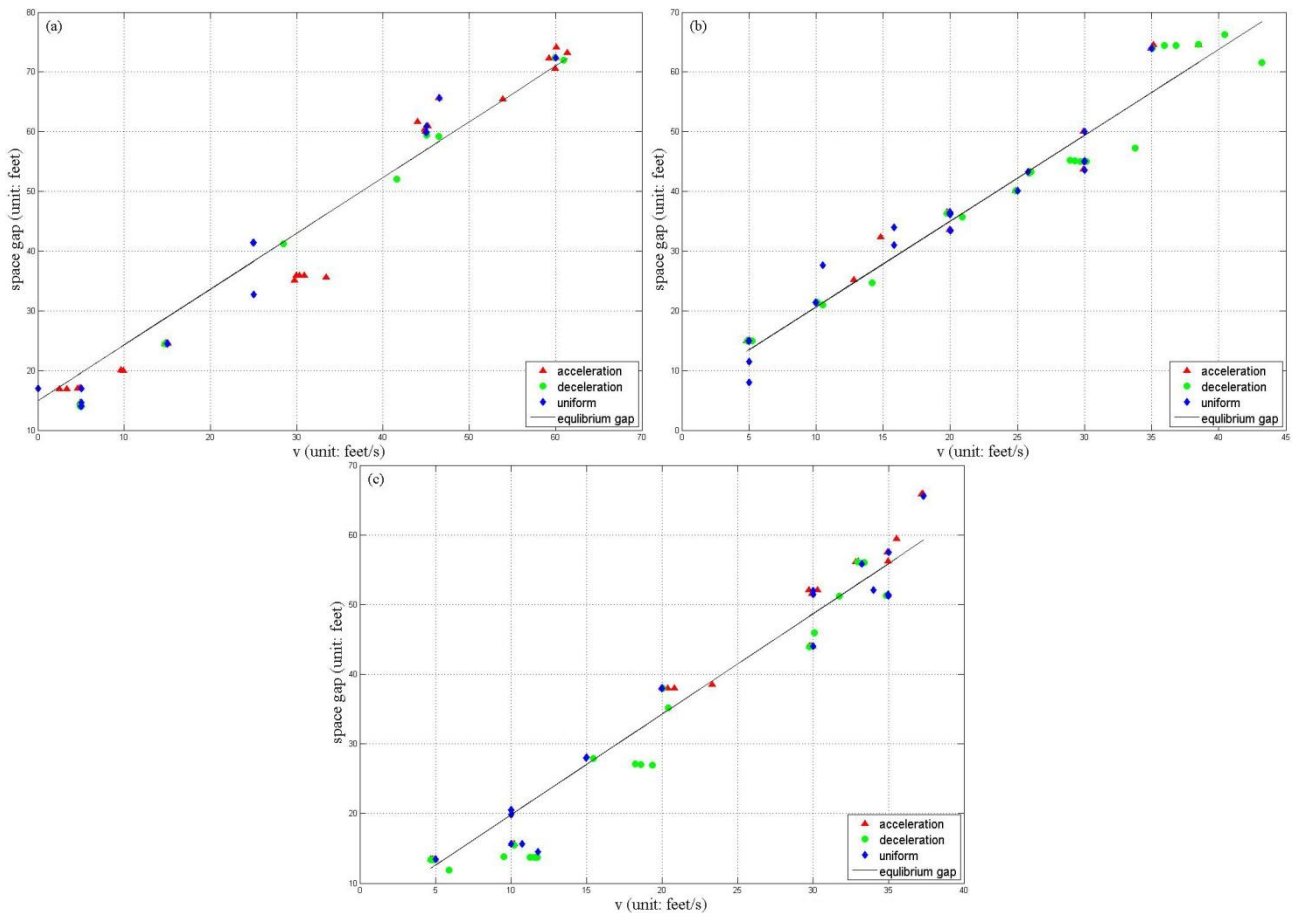
1. The vehicle's leading car could not change during the whole period, which means no lane change happens.
2. The sample size for the selected vehicle should be greater than 100.
3. The space headway should be shorter than $76m(250ft)$, since the distance between the two cars becomes too large, there will be no interaction (Bham and Benekohal, 2004).

After application these criteria, 323 vehicles were included in the analysis. The optimal values of T and s_0 for separate vehicles were estimated by the linear regression analysis. Some results are shown in Fig.2 and 3. The linear relationship between actual space gap s and speed v are identified when the speed difference $\Delta v \rightarrow 0$. Fig.2 and 3 also illustrate that vehicles will not keep uniform speeds although the actual space gap s approximates desired space gap s^* calculated by $s^* = s_0 + vT$ and speed difference Δv approximates zero. It means even the stimulus vanish,

1 i.e. $\Delta v \rightarrow 0$ and $s \rightarrow s^*$, vehicles accelerate or decelerate most of the time. Maybe, this could be explained by
 2 introducing drivers' anticipation or finite reaction effect into car following models. However, the following
 3 assumptions is made to explain this phenomenon from other perspective: *In the noiseless limit, vehicles' space gap*
 4 *will fluctuate around the desired space gap, rather than keep the desired space gap, in the homogeneous congested*
 5 *traffic flow.* In this perspective, no steady states exist in the homogeneous congested traffic flow. This is different from
 6 the fundamental diagram approach or the three-phase theory, which admit the existence of steady states. In this
 7 perspective, even if the actual space gap equals the desired space gap and speed difference equals approximates zero,
 8 vehicles will accelerate or decelerate stochastically. It should be noted that many car following models considered
 9 very small fluctuations around the desired space gap, i.e. acceleration noise. However, it is impossible that the
 10 acceleration noise is responsible for the high values of acceleration and deceleration in Fig.3.

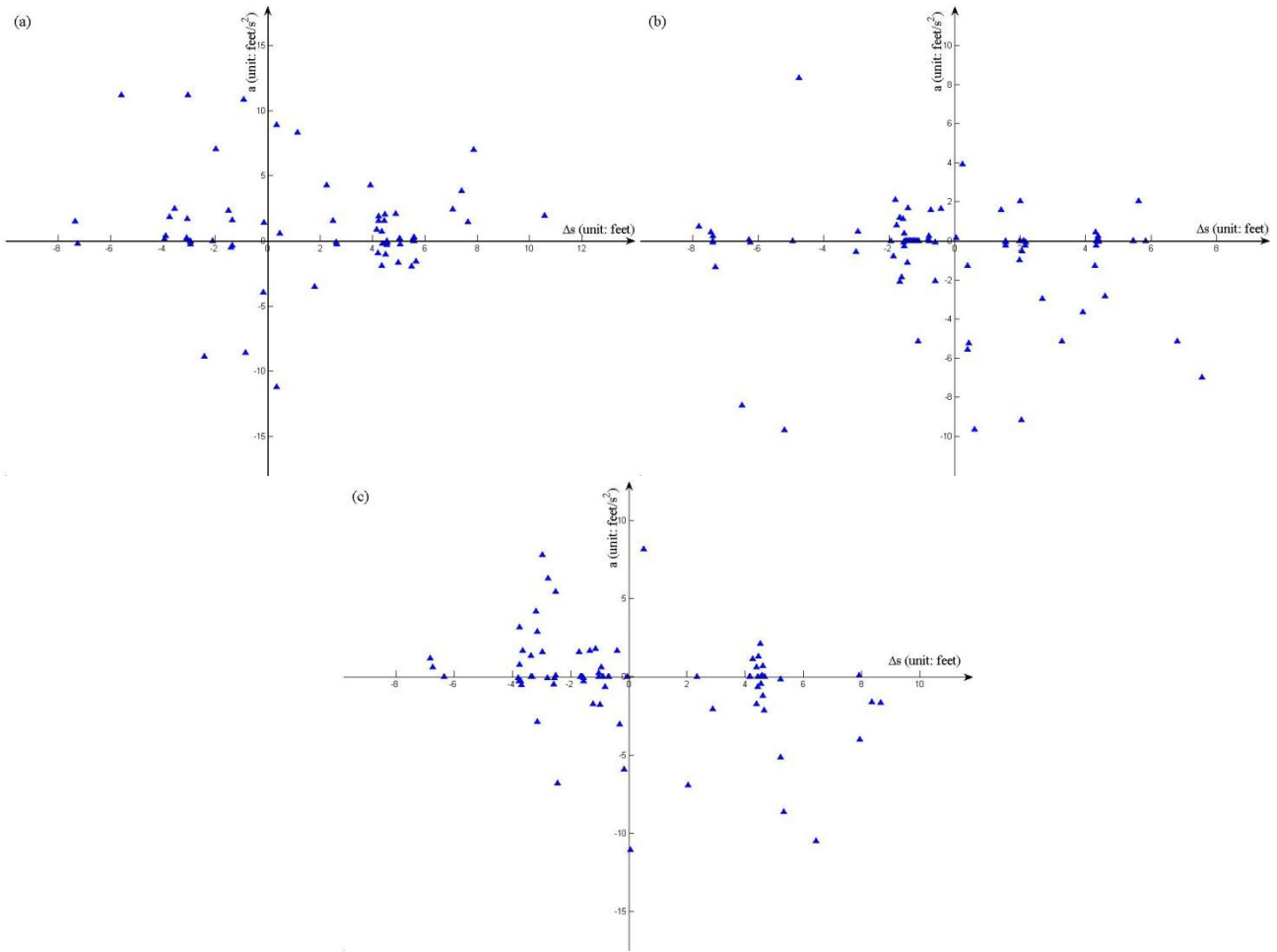


11
 12 **Fig. 1.** Sketch of US-101 study area.
 13



14
 15
 16 **Fig. 2.** Linear regression analysis for speed and space gap. (a-c) are single vehicle data taken from different detecting time interval 7:50

1 a.m. to 8:05 a.m., 8:05 a.m. to 8:20 a.m., and 8:20 a.m. to 8:35 a.m., respectively. If the acceleration or deceleration are less than
 2 $0.1m/s^2$, vehicles' speed is identified as the uniform speed.



3

4
 5 **Fig. 3.** The acceleration corresponding to Fig.2(a-c), respectively. $\Delta s = s - s_0 - vT$ and s is the actual space gap.
 6

7 F-Tests for significance at the level of 5% percent level are also performed when the linear relationship between
 8 space gap and speed are determined. The results are shown in Tab. 2 and Fig.4. Tab. 2 declares that almost all data
 9 indicate the existence of the linear relationship, although some values of s_0 are less than zero. If the data whose
 10 lower 95% confidence bounds of s_0 that less than zero are exclude, there still are 265(82%) samples remained.
 11

12 **Table 2**
 13 Overview of F-Tests of the linear relationship between space gap and speed.

Time interval	Number of simples available before testing for significance	Number of simples available after testing for significance	
		s_0	lower 95% confidence bounds of s_0 that greater than zero
07:50am-08:05am	84	84	74
08:05am-08:20am	98	97	78
08:20am-08:35am	141	139	113
Total	323	320	265

14

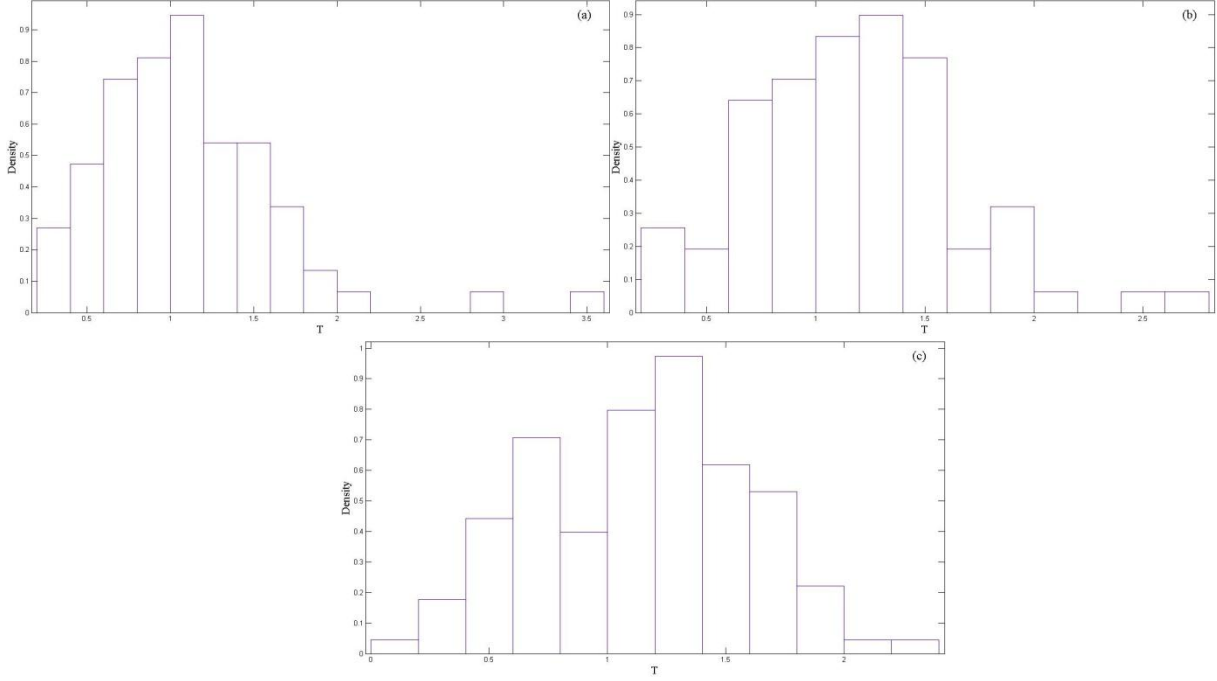


Fig. 4. Histogram of the safe time gaps.

3. The new model

Based on the above assumption, i.e., vehicles' space gap will fluctuate around the desired space gap in the homogeneous congested traffic flow in the noiseless limit, a cellular automaton model are proposed. The main mechanisms to incorporate this assumption are embodied in the randomization process of vehicles. The parallel update rules are as follows.

1. Determination of the randomization parameter $p_n(t+1)$ and deceleration extent Δv :

$$p_n(t+1) = \begin{cases} p_a : & \text{if } d_n^{eff}(t) < d_n^*(t) \\ p_b : & \text{if } v_n(t) = 0 \text{ and } t_n^{st}(t) \geq t_c \\ p_c : & \text{in all other cases} \end{cases} \quad (2)$$

$$\Delta v(t+1) = \begin{cases} dec : & \text{if } d_n^{eff}(t) < d_n^*(t) \\ 1 : & \text{in all other cases} \end{cases} \quad (3)$$

2. Acceleration:

$$v_n(t+1) = \min(v_n(t) + 1, v_{max})$$

3. Deceleration:

$$v_n(t+1) = \min(d_n^{eff}(t), v_n(t+1))$$

4. Randomization with probability $p_n(t+1)$:

$$\text{if } (rand() < p_n(t+1)) \text{ then } v_n(t+1) = \max(v_n(t+1) - \Delta v(t+1), 0)$$

5. The determination of $t_n^{st}(t+1)$:

$$\text{if } (v_n(t+1) = 0) \text{ then } t_n^{st}(t+1) = t_n^{st}(t) + 1$$

$$\text{if } (v_n(t+1) > 0) \text{ then } t_n^{st}(t+1) = 0$$

6. Car motion:

$$x_n(t+1) = x_n(t) + v_n(t+1)$$

where $d_n(t)$ is the space gap between vehicle n and its preceding vehicle $n+1$,

$d_n(t) = x_{n+1}(t) - x_n(t) - L_{veh}$, $x_n(t)$ is the position of vehicle n (here vehicle $n+1$ precedes vehicle n) and L_{veh} is the length of the vehicle, $v_n(t)$ is the velocity of the vehicle n . $d_n^*(t) = Tv_n(t)$ is the effective desired space gap between vehicle n and $n+1$, and T is the effective safe time gap between vehicle n and $n+1$ at the steady state. $d_n^{eff}(t)$ is the effective gap, $d_n^{eff}(t) = d_n(t) + \max(v_{anti}(t) - gap_{safety}, 0)$. $v_{anti} = \min(d_{n+1}(t), v_{n+1}(t) + 1, v_{max})$ is the expected velocity of the preceding vehicle in the next time step, and gap_{safety} is the safe distance that bigger than or equal to the randomization deceleration dec . The velocity anticipation effect is considered in order to reproduce the real time headway distribution, which has a cut off at the small time headway less than one second (Neubert et al., 1999). $t_n^{st}(t)$ denotes the time that a car stops.

The basis of the new model is the rules of the NaSch model with randomization parameter p_c to which a slow-to-start rule and the effective desired space gap $d_n^*(t)$ has been added. The slow-to-start effect is characterized by an increase of the randomization parameter from p_c to p_b ($> p_c$), which is the element to realize the $S \rightarrow J$ transition. The new model assumes the driver tends to keep $d_n^*(t)$ between vehicle n and $n+1$. When the effective gap $d_n^{eff}(t)$ is larger than $d_n^*(t)$, the driver will become defensive. The actual behavioral change is characterized by increasing the spontaneous braking probability from p_c to p_a . Moreover, the associated deceleration will change from 1 to dec (≥ 1). This effect is the factor to reproduce the transition from free flow to synchronized flow in new model.

In the following, the steady states of the new model are analyzed in the unperturbed, noiseless limit. For microscopic traffic flow models, the steady state requires that the model parameters are the same for all drivers and vehicles. In that case, the steady-state is characterized by the following two conditions (Treiber and Kesting, 2013):

1) *Homogeneous traffic*: All vehicles move at the same speed and keep the same gap behind their respective leaders.

2) *No accelerations*: all vehicles keep a constant time dependent speed.

Since the mechanisms associated with the hypothetical congested steady state analysis are all embodied in the randomization process, the noiseless limit should be taken as $p_a = 1, p_c = 0, p_b = 0$ or $p_a = 1, p_c = 1, p_b = 1$. However, all vehicles will keep a constant speed no matter how far distance between vehicles in the latter case, which is obviously unrealistic. Thus, we consider the former. According to the model rules, if $d^{eff}/T \geq v_{max}$, all vehicles will move with v_{max} ; if $d^{eff}/T < v_{max}$, all vehicles' speed will take turns to change simultaneously over time between $\max(v - dec, 0)$ and v , where $v \in [d^{eff}/T, \min(v_{max}, d^{eff})]$ and $\max(v - 1, 0) < d^{eff}/T$. It means there are no steady states of congested traffic in the new model. Vehicle's space gaps fluctuate around the desired gap. It means fluctuations are the internal Randomness of the drivers, not due to the driver heterogeneity, which is consistent with the empirical findings by Wagner (2012). Thus, this model is named as the cellular automaton model with non-hypothetical congested steady state (NH model). Furthermore, if the acceleration rule in NH model is revised as follows, the cellular automaton model within the fundamental diagram approach can be obtained:

$$\text{if } d_n^{eff}(t) > d_n^*(t) \text{ then : } v_n(t+1) = \min(v_n(t) + 1, v_{max}) \quad (4)$$

4 Simulation investigation

In this section, simulations are carried out on a road with length $L_{road} = 1000L_{cell}$. Both the cell length and vehicle length are set as $7.5m$, i.e. $L_{cell} = 7.5m$ and $L_{veh} = 1L_{cell}$. During the simulations, first 50000 time steps are discarded to let the transient time die out. The parameters are shown in Tab. 3.

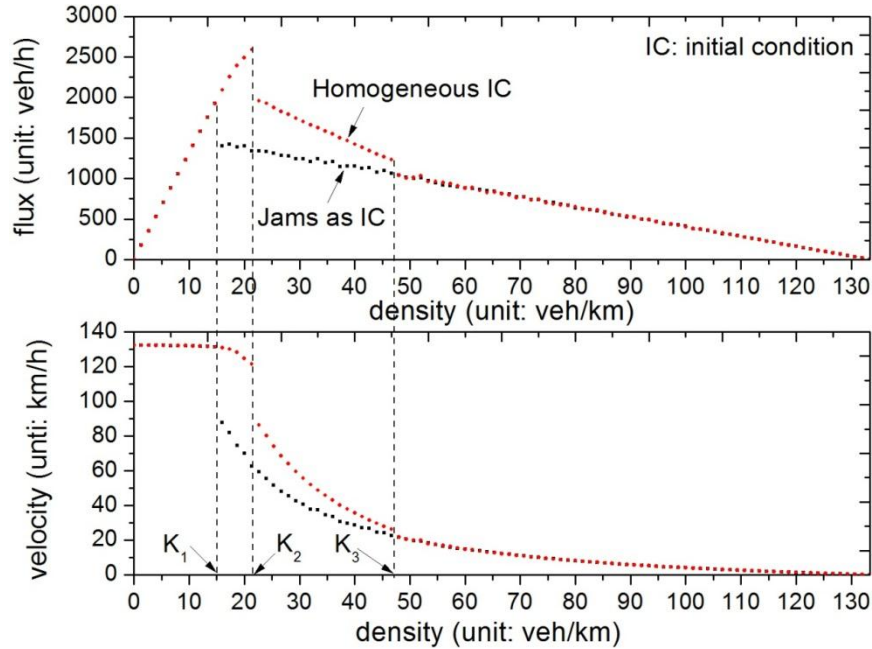
1 **Table 3**
 2 Model parameters.

Parameters	L_{cell}	L_{veh}	V_{max}	T	d	p_a	p_b	p_c	gap_{safety}	t_c
Units	m	L_{cell}	L_{cell}/s	s	L_{cell}/s^2	-	-	-	L_{cell}	s
Value	7.5	1	5	1.8	1	0.95	0.55	0.1	2	8

3
 4 **4.1. Periodic boundary condition**

5 Fig.5 shows the fundamental diagram of the model. One could see that there are two branches on the
 6 fundamental diagram in the density region $K_1 < K < K_3$: the upper branch is obtained from the initially
 7 homogeneous distribution of traffic whereas the lower starts from a wide moving jam. Therefore, three traffic phases
 8 and two first order transitions (the transitions from free flow to synchronized flow (F→S) and from synchronized
 9 flow to wide moving jams (S→J)) are clearly distinguished, exhibiting a typical double Z-characteristic structure
 10 predicted by the three-phase traffic flow theory. Moreover, when the density increasing ($K_2 < K < K_3$), the flux
 11 begins to decrease and the synchronized flow starts to emerge in the free flow when the initially state is homogeneous
 12 traffic (Fig.6(a),(b)). While the initially wide moving jams traffic will evolve to the state that wide moving jams and
 13 free flow coexist (Fig.6(c),(d)).

14 Next, we distinguish the synchronized flow and the wide moving jam phases with single traffic data. The flow
 15 interruption effect could be used as a criterion to distinguish the synchronized flow and wide moving jam phases (see
 16 Appendix). We obtained the data by setting a virtual detector on the road. The interruption effect can be clearly
 17 identified in Fig.7(a),(b). Before and after the wide moving jam has passed the detector, many vehicles traversed the
 18 detector. But within the jam, no vehicles traversed the detector, and the velocity within the jam is zero. This means
 19 that the traffic flow is discontinuous within the moving jam, i.e., this moving jam is associated with the wide moving
 20 jam phase. The flow interruption does not occur in Fig.7(c),(d). Thus, this is associated with the synchronized flow
 21 phase.



22
 23 **Fig. 5.** Space-averaged flow-density diagram of NH model. "Homogeneous IC" represents the initially homogenous distribution of traffic,
 24 and "Jams as IC" represents the initially wide moving jam distribution of traffic. The upper lines between K_2 and K_3 in the
 25 flux-density and speed-density plots, respectively, correspond to a mixture of coexisting free traffic and synchronized phases, while the
 26 lower line between K_1 and K_3 corresponds to a coexistence of free traffic and jams.

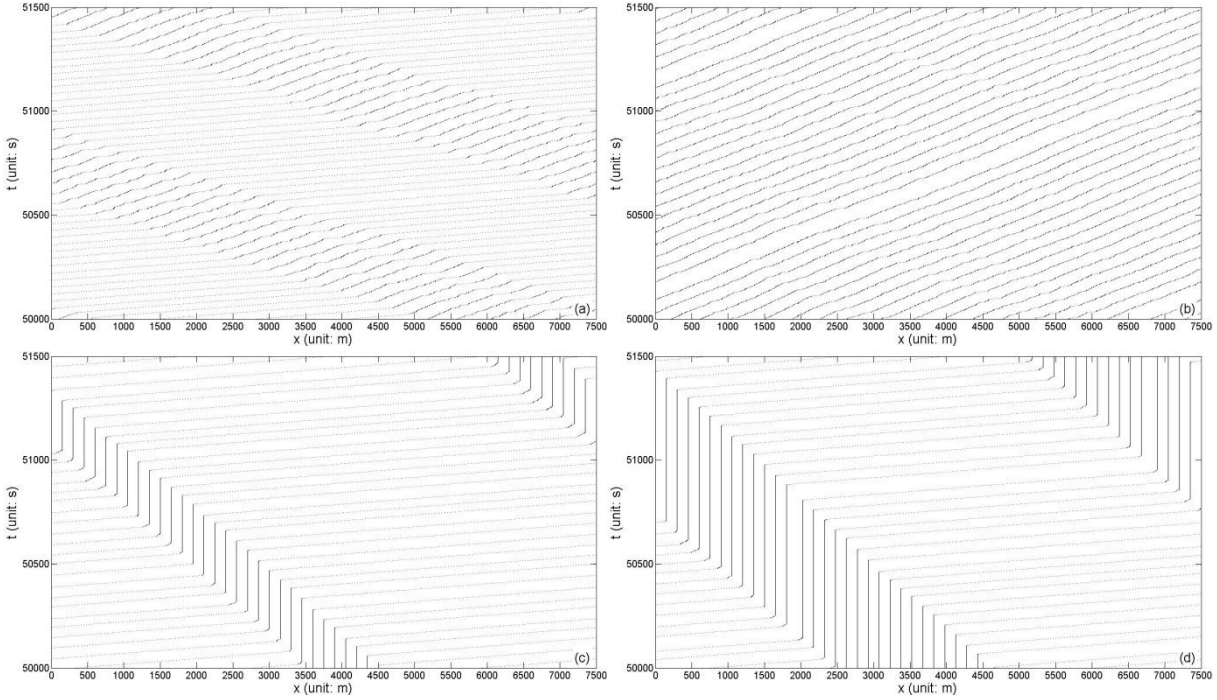


Fig. 6. The spatial-temporal diagrams of NH model, (a) $k=27$, (b) $k=47$, (c) $k=27$, (d) $k=47$ (unit: veh/km). (a, b) Starting from homogeneous initial state. (c, d) Starting from a wide moving jam initial state. The horizontal direction (from left to right) is space and the vertical direction (from down to up) is time.

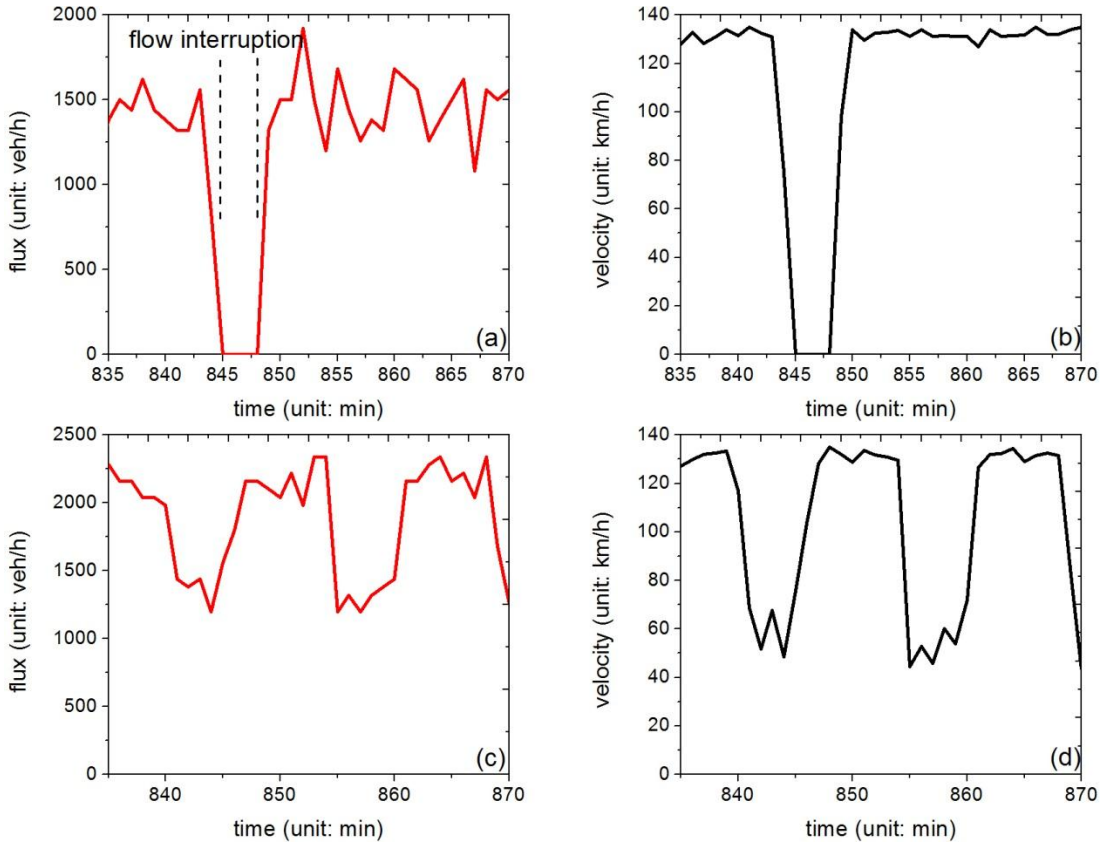


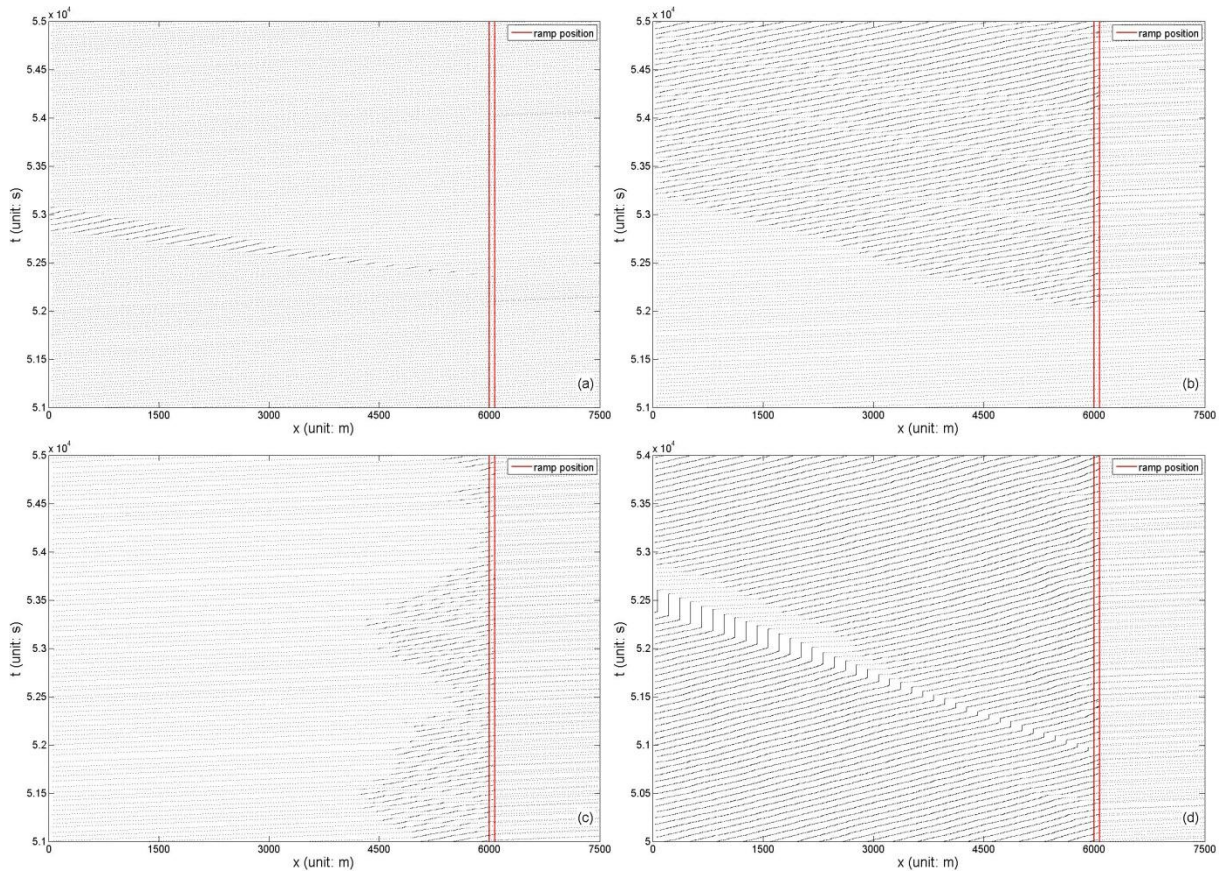
Fig. 7. (a), (c) The 1 min average flux. (b), (d) The 1 min average velocity. (a), (b) starting from a wide moving jam initial state responding to Fig. 6(c). (c), (d) starting from homogeneous initial state responding to Fig. 6(a).

1 4.2. Open boundary condition

2 The traffic patterns that emerge near an on-ramp are studied under open boundary condition. The vehicles drive
 3 from left to right. The left-most cell corresponds to $x = 1$. The position of the left-most vehicle is x_{last} and that of
 4 the right-most vehicle is x_{lead} . At each time step, if $x_{last} > v_{max}$, a new vehicle with velocity v_{max} will be
 5 injected to the position $\min(x_{last} - v_{max}, v_{max})$ with probability q_{in} . If $x_{lead} > L_{road}$, the leading vehicle will be
 6 removed and the following vehicle becomes the leader.

7 We adopt a simple method to model the on-ramp. Assuming the position of the on-ramp is x_{on} , a region
 8 $[x_{on} - L_{ramp}, x_{on}]$ is selected as the inserting area of the vehicle from on-ramp. At each time step, we find out the
 9 longest gap in this region. If the gap is large enough for a vehicle, then a new vehicle will be inserted at the cell in the
 10 middle of the gap with probability q_{on} . The velocity of the inserted vehicle is set as the velocity of its preceding
 11 vehicle, and the stop time is set to zero. In this paper, the parameters are set as $x_{on} = 0.8L_{road}$ and
 12 $L_{ramp} = 10L_{cell}$.

13



14

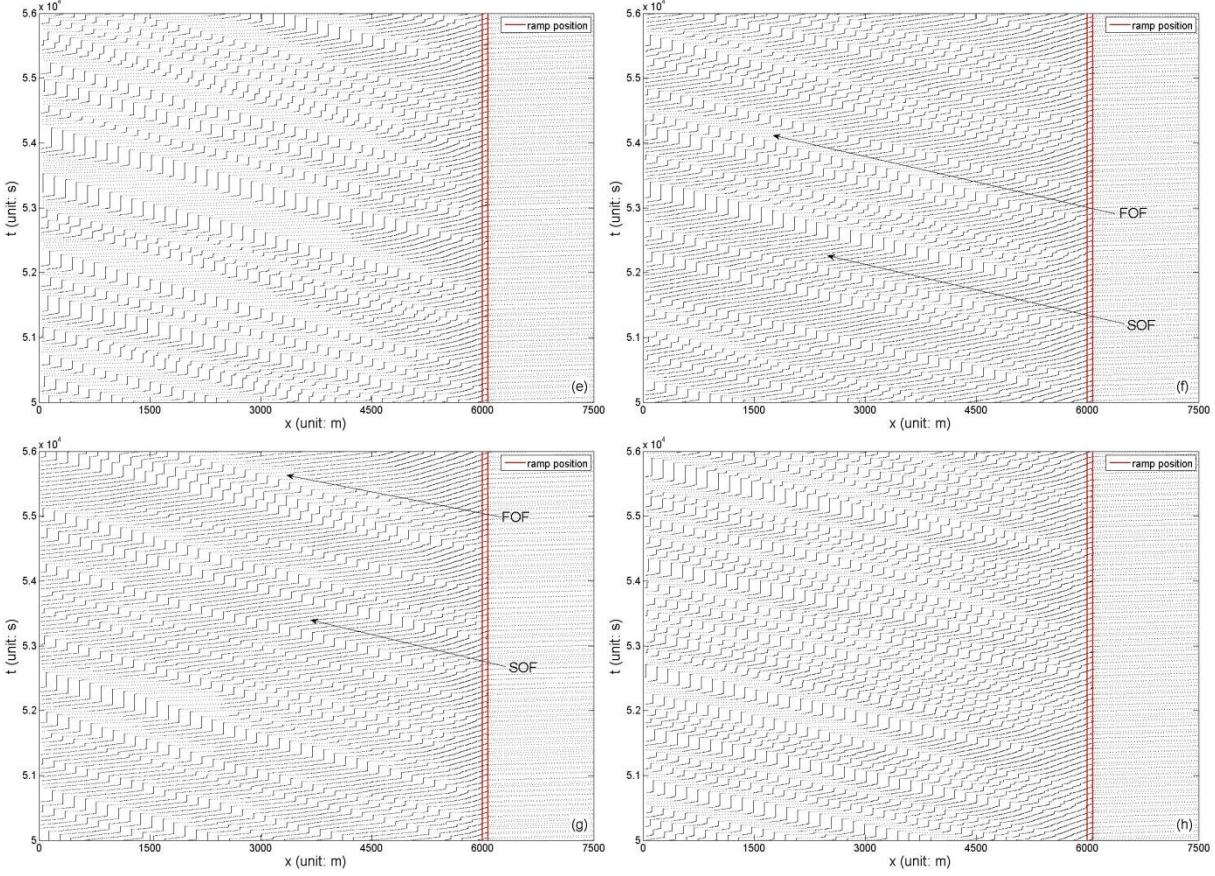


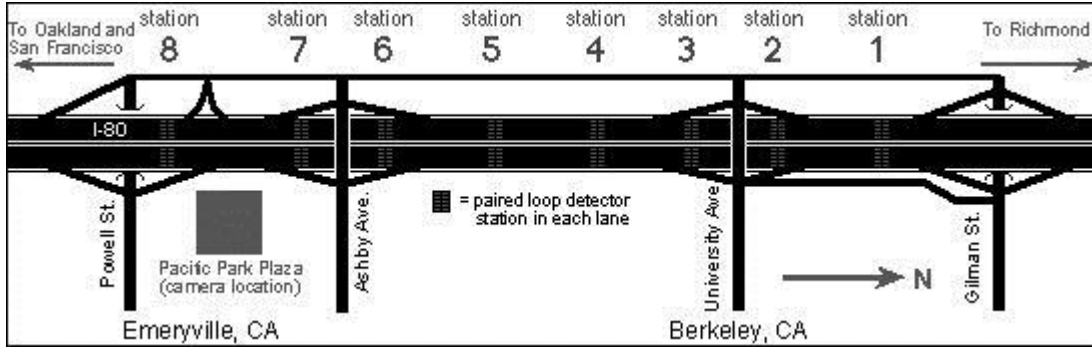
Fig. 8. The spatial-temporal diagrams of the congested patterns. (a) $q_{in} = 2339, q_{on} = 19$ (MSP), (b) $q_{in} = 1728, q_{on} = 968$ (WSP), (c) $q_{in} = 1440, q_{on} = 823$ (LSP), (d) $q_{in} = 1134, q_{on} = 1123$ (DGP), (e) $q_{in} = 920, q_{on} = 1304$ (GP), (f) $q_{in} = 931, q_{on} = 1304$ (GP), (g) $q_{in} = 933, q_{on} = 1011$ (GP), (h) $q_{in} = 907, q_{on} = 1410$ (GP) (unit: veh/h). The horizontal direction (from left to right) is space and the vertical direction (from down to up) is time. (f) $P_b = 0.5$, (g) $P_b = 0.55, T = 1.6, gap_{safety} = dec = 2$, (h) the acceleration rule is according to equation (4). 'SOF' and 'FOF' represent the synchronized outflow and free outflow of wide moving jams, respectively.

In Fig.8(a), the spatial-temporal features of the congested pattern named moving synchronized flow (MSP) reproduced are shown. In this pattern, synchronized traffic flow spontaneously emerges in the free flow. Fig.8(b) exhibits the widening synchronized flow (WSP). For this pattern, wide moving jams do not emerge in synchronized flow. The downstream front of WSP is fixed at the on-ramp and the upstream front of WSP propagates upstream continuously over time. In Fig.8(c), both the downstream and the upstream front of synchronized flow are fixed at the on-ramp, thus, it belongs to the local synchronized pattern (LSP). Moreover, the width of LSP in the longitudinal direction changes over time, which is in accordance with empirical observations. Fig.8(d) shows the dissolving General Patterns (DGP) in which just one wide moving jam emerges in the synchronized flow. Fig.8(e) shows the spatial-temporal features of General Pattern (GP). Only free outflow exists in the downstream of wide moving jams in GP, which has been criticized by the three-phase theory. However, it can be easily improved if we decrease the slow-to-start probability p_b or adjust the values of T and dec , see Fig.8(f, g). Thus, all the above simulation results are well consistent with the well-known results of the three-phase traffic theory. However, if the acceleration rule is revised as equation (4), the synchronized outflow cannot be reproduced any more.

5. Empirical validation

In order to validate NH model, comparing the simulating data with the empirical data is necessary. The datasets

1 presented by NGSIM are from double loop detectors between Powell Street and Gilman Avenue on Interstate 80 (I-80)
 2 in Emeryville, California, see Fig.9. The data were collected through Freeway Performance Measurement System
 3 (PeMS) project, which was conducted by the Department of Electrical Engineering and Computer Sciences at the
 4 University of California, at Berkeley, with the cooperation of California Department of Transportation. Available data
 5 from six detector stations (Stations 1, 3, 4, 5, 6 and 7) were provided in this data set. Each detector station contains
 6 two detectors per lane. NH model will be calibrated with the data of Thursday, 07 Apr 2005 and then validated with
 7 the data of other five days.

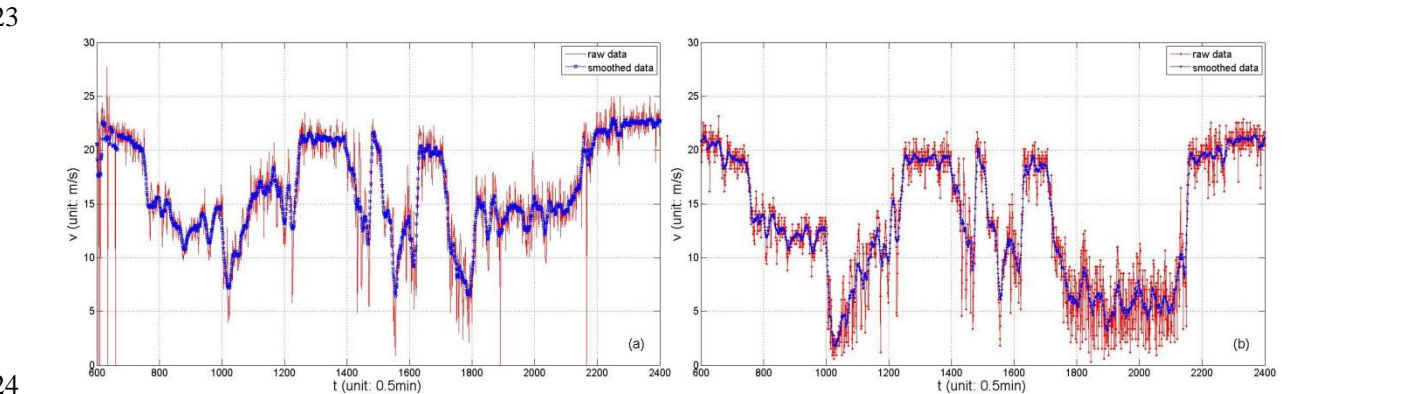


8 **Fig. 9.** Sketch of I-80 near Berkeley.

9
 10
 11 Since NH model is a single-lane model, the method of Brockfeld et al. (2005) is applied to conduct the
 12 simulations. The data from loop detectors at three stations, Stations 4, 5, and 6, are chosen, which cover a segment of
 13 1067m without an on-ramp but one less used off-ramp. The multi-lane data is averaged as a single lane data to avoid
 14 the additional complexity of lane-change rules needed to perform multi-lane simulation. Free traffic and synchronized
 15 flow can be identified in Fig.10 (a-e), which shows the time series of speed for each lane at Station 5 on Thursday,
 16 07 April 2005. Fig.10(f) is the average speed (v_{ave}^5) data on the station 5, derived from the following equation:

$$17 \quad v_{ave}^i = \frac{\sum_{j=1}^N v_{ij}^{emp} f_{ij}^{emp}}{\sum_{j=1}^N f_{ij}^{emp}} \quad (5)$$

18 where f_{ij}^{emp} and v_{ij}^{emp} are the flux and velocity of lane j detected by the station i . Comparing with Fig.10(a-e),
 19 Fig.10(f) is capable of reflecting the real situation around Station 5. Thus, it can be used to test whether the new model
 20 can describe the real complex traffic flow patterns. Since the speed of synchronized flow fluctuates widely, the data is
 21 smoothed by moving average filter provided by MATLAB with the span set as 15, to identify the variation trends of
 22 traffic flow more intuitively.



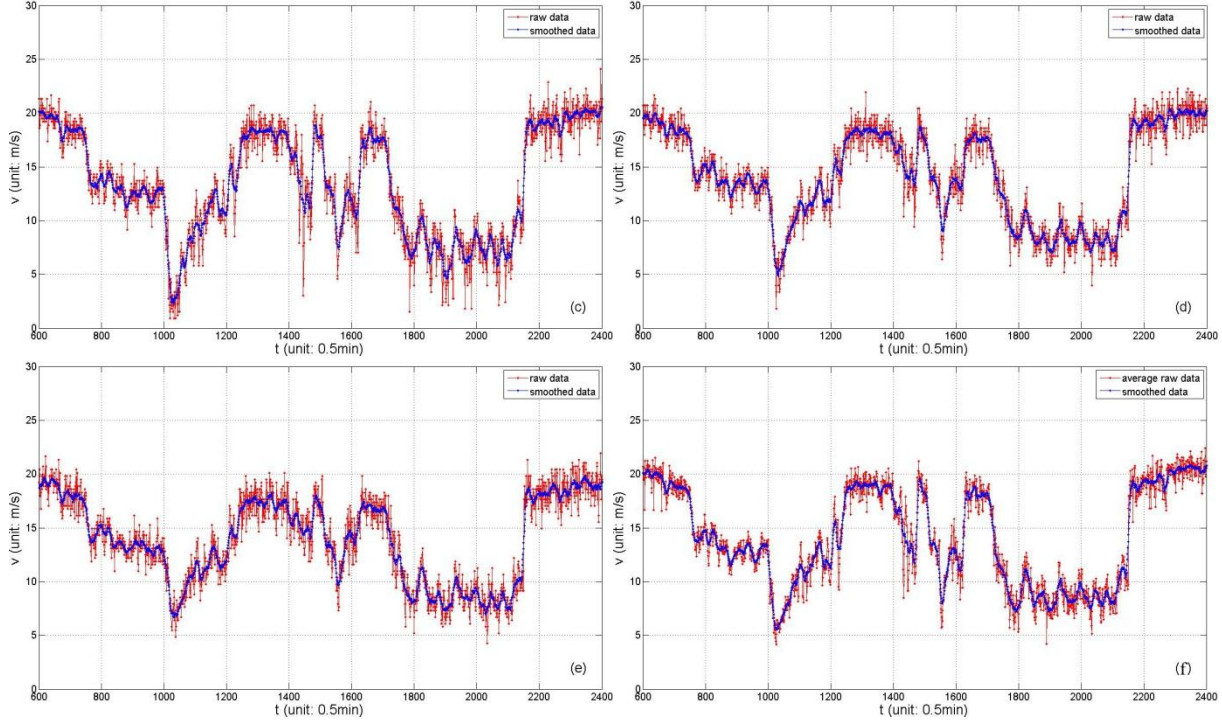


Fig. 10. Real Time series of speed at Station 5 on Thu, 07 Apr 2005.

5.1. Simulation setup

The vehicles are generated at inflow Station 4. To insert new vehicles, we define an entrance section upstream of Station 4. The position of Station 4 is $x = 0$ and its upstream region is located at $x < 0$. If there are no vehicles in the upstream region of Station 4, a new vehicle is generated with the probability q_{in} , where q_{in} is calculated according to the measured flow q_{ave}^A in the 30s interval at Station 4, i.e. $q_{in} = q_{ave}^A/30$. The speed and location of the vehicle to be inserted are set to the speed of the its leading vehicle $v_{leading}$ and $-v_{leading}$, respectively.

To regulate the outflow, the limit speed region closely downstream of Station 6 is defined, which starts from the position of Station 6, and ends with the length $L_{sl} = 50m$. In the speed limit region, a dynamic speed limit is applied, which equals the velocity v_{ave}^6 that Station 6 measured. Since the CA models require an integer value for the speed limit, we converted the value to $\lfloor v_{de}/L_{cell} + 1 \rfloor$, where $\lfloor x \rfloor$ denotes the maximum integer that is not bigger than x .

5.2. Good-of-fit measures

Theil's inequality coefficient (U) is applied to measure the performance (Brockfeld et al., 2005; Ahmed, 1999), which is defined as follows:

$$U = \frac{\sqrt{\frac{1}{N} \sum_i (v_i^{empi} - v_i^{simu})^2}}{\sqrt{\frac{1}{N} \sum_i (v_i^{empi})^2} + \sqrt{\frac{1}{N} \sum_i (v_i^{simu})^2}} \quad (6)$$

where v_i^{simu} is the i th speed of the simulation data. The value of U always falls between 0 and 1. $U = 0$ implies a perfect fitness. Related to the Theil's inequality coefficient, the bias (U^M) and the variance (U^S) are often applied:

$$U^M = \frac{(\mu_{v_{empi}} - \mu_{v_{simu}})^2}{\frac{1}{N} \sum_i (v_i^{empi} - v_i^{simu})^2} \quad (7)$$

$$U^S = \frac{(\sigma_{v_{empi}} - \sigma_{v_{simu}})^2}{\frac{1}{N} \sum_i (v_i^{empi} - v_i^{simu})^2} \quad (8)$$

where $\mu_{v_{empi}}$, $\mu_{v_{simu}}$, $\sigma_{v_{empi}}$ and $\sigma_{v_{simu}}$ are the means and standard deviations of the empirical and the simulated speed series respectively. The bias proportion (U^M) reflects the systematic error. The variance proportion (U^S) indicates how well the fluctuation in the original data is replicated by the simulation. Therefore, lower values (close to zero) of U^M and U^S are desired.

5.3. Calibration

In contrasted to previous works, such as (Brockfeld et al., 2005), the automated calibration methods are not used, since they will not always obtain the satisfied results. Moreover, parameters in NH model can be calibrated in a very simple way, after the cell length L_{cell} is determined. The maximum velocity V_{max} could be observed by the empirical data. Through the average free flow speed v_{free}^{ave} , the randomization probability p_c is calculated by $v_{free}^{ave} = V_{max} * (1 - p_c)$. The randomization probability p_b can be estimated by $v_g = -(1 - p_b)/k_{max}$ if the downstream propagation velocity of the wide moving jam v_g is determined, where k_{max} is the density inside the jam. Rehborn et al. (2011) have discussed several methods to measure v_g , and gives its value interval $[-18, -10]km/h$ (Treiber et al. (2010) give the interval $[-20, -15]km/h$). Another wide moving jam related parameter t_c affects the wide moving jam emergence. Given fixed p_b , larger t_c can make heavier synchronized flow can be maintained, i.e., reduce probability emergence of the wide moving jam in synchronized flow (Jiang and Wu, 2003). The parameter gap_{safety} is no smaller than the deceleration dec to keep safety, and influences the maximum flux of free flow. A simple way is to set $gap_{safety} = dec$. Furthermore, we found it is best not and unnecessary to change the value of randomization probability p_a . Thus, only L_{cell} , L_{veh} , T and dec are left to be adjusted, which influence the state of the synchronized flow. Moreover, one cell could just occupied by one vehicle in cellular models, i.e. $L_{veh} = mL_{cell}$, m is an integer. The trial and error method is adopted to determine their values.

During the simulations, we found smaller cell length L_{cell} is needed to make the simulation data more consistent with the empirical data and $L_{cell} = 2.5m$ is good enough to obtain satisfactory results. Since the maximum velocity measured by the detectors is around $20m/s$, Thus, the maximum velocity is set as $V_{max} = 8L_{cell}/s$. As the vehicle types and length is unknown, only one type of vehicles with the length $L_{veh} = 3L_{cell}$ is assumed during the simulations. The wide moving jams have not been detected, so P_b and t_c will not change. Fig.11(a) is the results of keeping other parameters unchanged. Free flow always maintains, which means the synchronized flow in front is underestimated. Thus, we need to increase the values of T and dec . Moreover, Fig.10 shows that the speed in synchronized flow is widely fluctuate. Thus, bigger values should be assigned to T and dec .

The final optimal model parameters and U values are given in Tab. 4 and 5. Due to the stochastic nature of the model, separate runs of simulation with the optimal model parameters lead to different U values. Nevertheless, we found repeat runs only lead to slightly different U values. All the simulated speed series describe good agreement with the empirical data, see Fig.11(b, c), which is one run result.

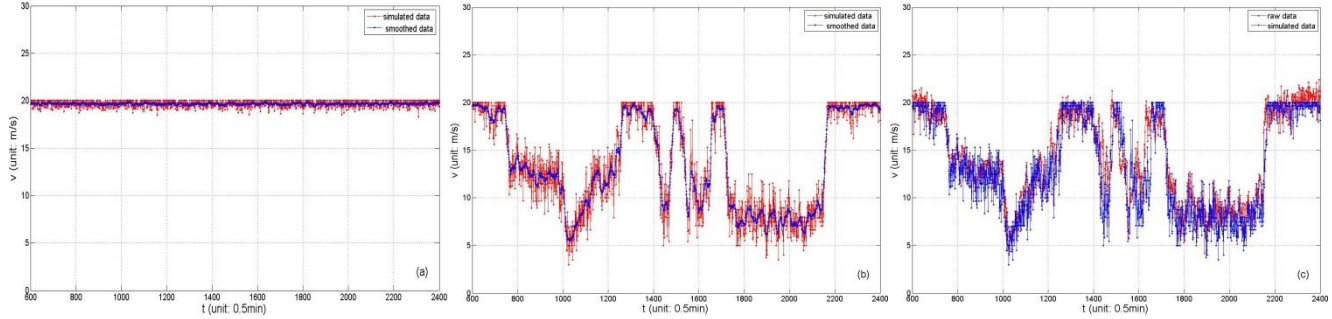
Table 4
Optimal model parameters.

Parameters	L_{cell}	L_{veh}	V_{max}	T	d	p_a	p_b	p_c	gap_{safety}	t_c
Units	m	L_{cell}	L_{cell}/s	s	L_{cell}/s^2	-	-	-	L_{cell}	s
Value	2.5	3	8	3.5	3	0.95	0.55	0.1	3	8

Table 5
Calibration and Validation Errors (U, U^M, U^S), corresponding to Fig.11-16.

Day	07 Apr	08 Apr	11 Apr	12 Apr	13 Apr	14 Apr
\bar{U}	0.0779	0.0864	0.0621	0.0591	0.059	0.0782
U^M	0.1018	0.0793	0.0414	0.065	0.1365	0.1596
U^S	0.0326	0.0065	0.0234	0.0339	0.0095	0.0011

1



2

3

Fig. 11. Simulated Time series of speed at Station 5 on Thu, 07 Apr 2005.

4

5

5.4. Validations

6

7

8

9

10

11

12

13

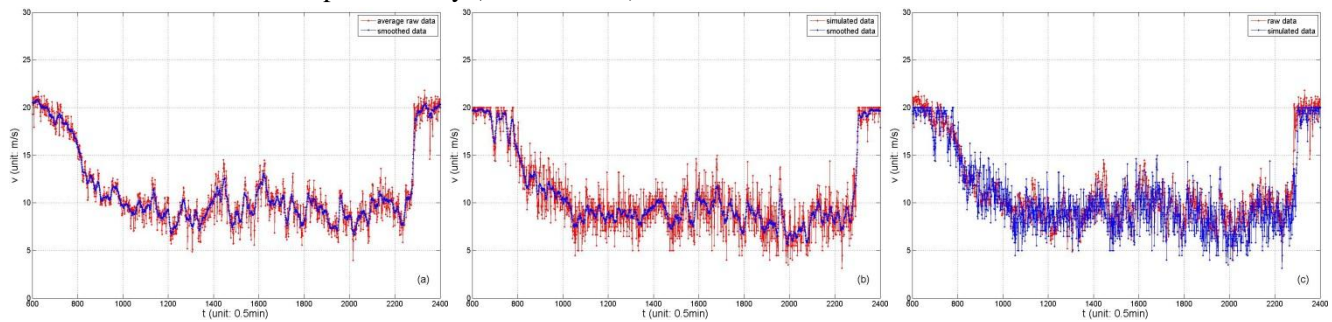
14

15

16

17

In order to study the robustness of the calibrated parameters, we validate the model using the data collected on other different days. The results are described in Fig.12-16 and Tab. 5. The validated results can capture traffic dynamics accurately on the first three days (08-12 Apr). On 13 and 14 Apr, U^M becomes larger than before, which can reflect the difference between the mean values of the data and the simulation. It can be shown in Fig.15 and 16 that the empirical speed are bigger than the simulated speed. Bigger value of maximum speed and smaller cell size may fix this deficiency. On the whole, all validation results are acceptable and better than the results of all models tested in by Brockfeld et al. (2005). Brockfeld et al. tested many models on the same location and the traffic dynamics are almost as complex as ours, which show that the U values of tested models are all bigger than 0.1. Moreover, it should be noted that our simulations are based on the homogeneous traffic and the heterogeneity is not considered, while real traffic flow is heterogeneous. Thus, the validation results mean that the real heterogeneous traffic can be simulated by the homogeneous traffic of NH model, which is highlighted as the one of the prominent advantages of the models within the three-phase theory (Kerner, 2012).

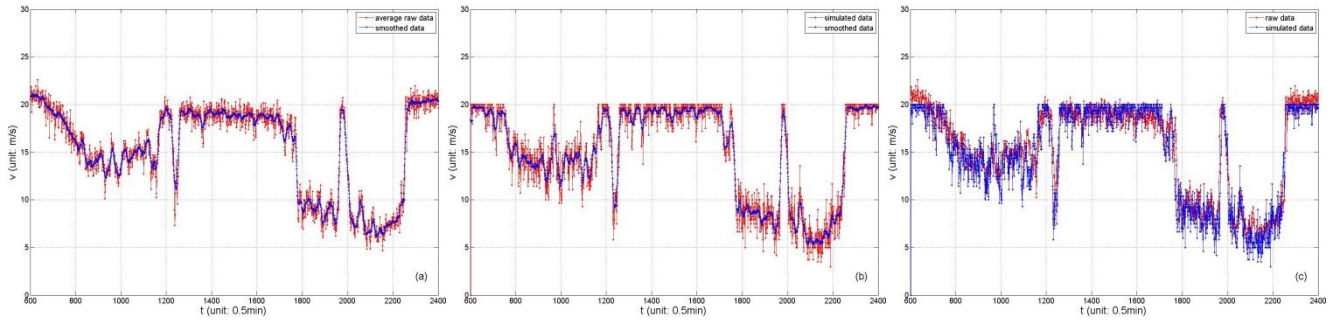


18

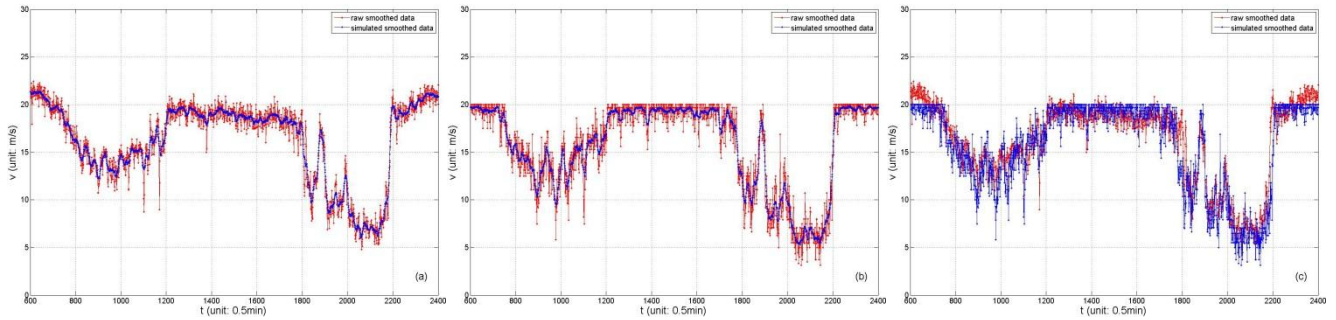
19

Fig. 12. Simulated Time series of speed at Station 5 on Fri, 08 Apr 2005.

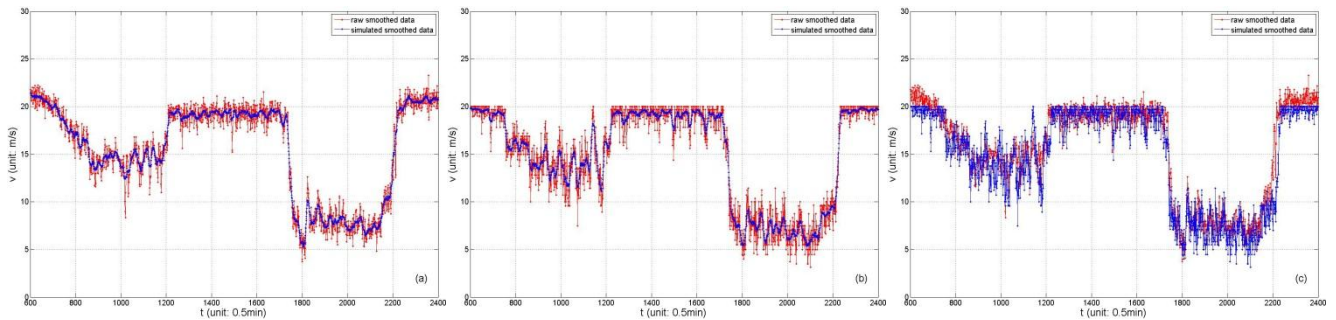
20



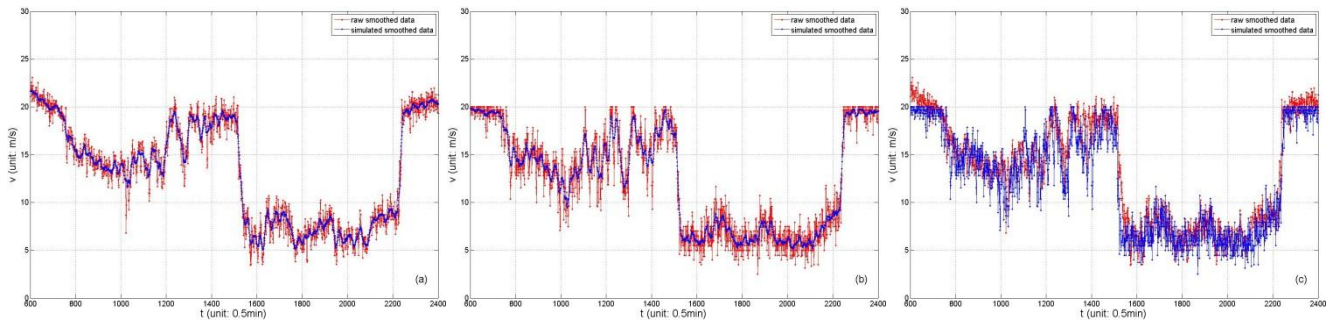
1
2
3
Fig. 13. Simulated Time series of speed at Station 5 on Mon, 11 Apr 2005.



4
5
6
Fig. 14. Simulated Time series of speed at Station 5 on Tue, 12 Apr 2005.



7
8
9
Fig. 15. Simulated Time series of speed at Station 5 on Wen, 13 Apr 2005.



10
11
12
Fig. 16. Simulated Time series of speed at Station 5 on Thu, 14 Apr 2005.

13 **6. Conclusion**

14 Traffic flow theory can be divided into two main branches, the fundamental diagram approach and the
15 three-phase theory. The fundamental diagram approach assume the existence of an unique space-gap-speed

1 relationship, while the three-phase theory presumes drivers can make arbitrary choice of the space gap within some
2 gap range.

3 In order to determine whether the unique space-gap-speed relationship exists, the US-101 trajectory datasets of
4 NGSIM are analyzed. Results showed the following findings in the 82% of the cases: (1) linear relationship between
5 actual space gap and speed can be identified when the speed difference between vehicles approximate zero; (2)
6 vehicles accelerate or decelerate around the desired space gap most of the time. To explain these phenomena, an
7 assumption and a new cellular model (NH model) are proposed that in the noiseless limit vehicles' space gap will
8 fluctuate around the desired space gap, rather than keep the desired space gap, in the homogeneous congested traffic
9 flow.

10 Two parts of simulations are conducted. In the first part, simulations on both a circular road and an open road
11 with an on-ramp were carried out for NH model. Results obtained under the periodic conditions show that NH model
12 could produce the synchronized flow and two kinds of phase transitions, i.e. F→S transition and S→J transition.
13 Results obtained from an open road with an on-ramp show that multiple congested patterns observed by the
14 three-phase theory can be well reproduced by NH model. In the second part, NH model has been calibrated and
15 validated by the I-80 detector datasets of NGSIM. Results show that the empirical data can be well reproduced and the
16 validation errors are smaller than previous studies.

18 **Acknowledgements:**

19 The authors wish to thank NGSIM for supplying the empirical data used in this article. Tian sincerely thanks for
20 the help of Guojun Jiang and Yang Xu to deal with the empirical data. This work is supported by the Fundamental
21 Research Funds for the Central Universities (2013YJS052), the 973 Program (No. 2012CB725403), and the National
22 Natural Science Foundation of China (Grant Nos.71222101, 71071013).

24 **Appendix: The three-phase theory**

25 *A.1. Congested traffic phases*

26 In three-phase theory, congested traffic has been divided into the synchronized flow and wide moving jam phases,
27 which are defined through empirical criteria [S] and [J]:

28 Wide moving jams [J]: A wide moving jam is a moving jam that maintains the mean velocity of the downstream jam
29 front, even when the jam propagates through other traffic phases or bottlenecks. Within the downstream front of the
30 wide moving jam, vehicles accelerate from the standstill inside the jam to free flow. Within the wide moving jam, the
31 vehicles are almost in a standstill or if they are moving, their speeds are very low. Within the upstream front of the
32 wide moving jam vehicles must slow down to the speed within the jam. Generally, if the width of a moving jam (in
33 the longitudinal direction) considerably exceeds the width of the jam fronts, one could call it a wide moving jam.

34 The synchronized flow phase [S]: In contrast with the wide moving jam phase, the downstream front of the
35 synchronized flow phase does not exhibit the wide moving jam characteristic feature; in particular, the downstream
36 front of the synchronized flow phase is often fixed at a bottleneck. In synchronized flow, the average speed of vehicles
37 is noticeably lower and the density of vehicles is noticeably higher than the corresponding values in free traffic at the
38 same flux of vehicles.

39 The criterion [J] could be explained by a flow interruption effect within a wide moving jam that occurs when
40 vehicles are in a standstill or move with negligible low speed within the jam. A sufficient criterion for this flow
41 interruption effect is:

$$42 \quad T_{max} \gg T_{del}^{(ac)} \quad (9)$$

1 where T_{max} is the maximum time headway between two vehicles within the jam and $T_{del}^{(ac)}$ is the mean time
 2 delay in vehicle acceleration at the downstream jam front from a standstill state within the jam. In a hypothetical case,
 3 when all vehicles within a moving jam do not move, the criterion for this flow interruption effect is:

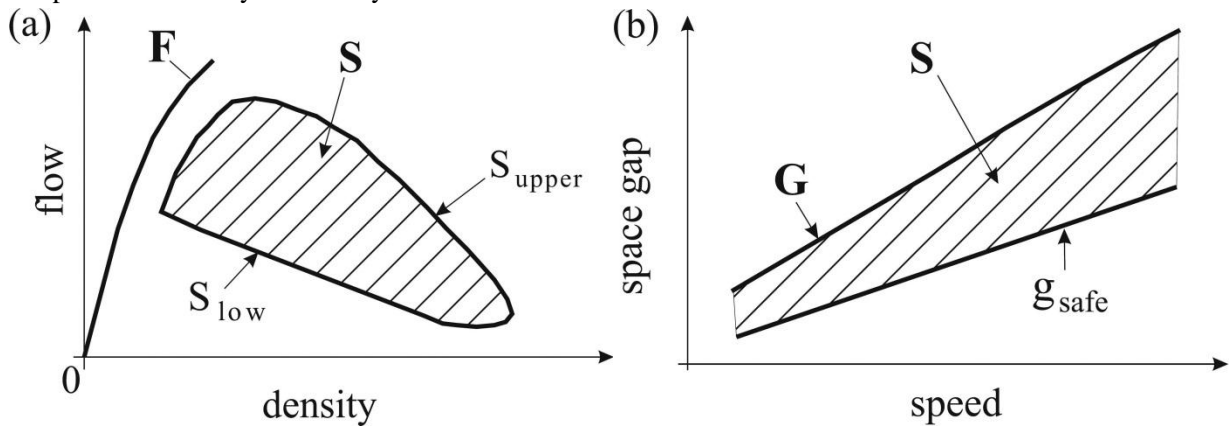
$$4 \quad T_J \gg T_{del}^{(ac)} \quad (10)$$

5 where T_J is the jam duration, i.e. the time interval between the upstream and downstream jam fronts passing a
 6 detector location.

7 Condition (9) indicates that vehicles inside the moving jam is at least once in a stop during a large time interval
 8 compared with the mean time delay in vehicles acceleration from standstill at the downstream front. Under condition
 9 (9), there are at least several vehicles within the jam that are in a standstill or if they are still moving, it is only with a
 10 negligible low speed in comparison with the speed in the jam inflow and outflow. These vehicles could separate
 11 vehicles accelerating at the downstream jam front from vehicles decelerating at the upstream jam front. Therefore the
 12 jam inflow has no influence on the jam outflow, and the jam outflow only depends on the vehicles that accelerating
 13 from standstill at the downstream front. Thus, the traffic flow interruption effect can be used as a criterion to
 14 distinguish between the synchronized flow and wide moving jam phases in single vehicle data.
 15

16 A.2. The fundamental hypothesis of the three-phase traffic theory

17 The fundamental hypothesis of the three-phase theory is as follows: the hypothetical steady states of the
 18 synchronized flow cover a two-dimensional region in the flow-density plane, i.e., there is no fundamental diagram of
 19 traffic flow in this theory, Fig.A.1. The steady state of synchronized flow is a hypothetical state of synchronized flow
 20 of identical vehicles and drivers in which all vehicles move with the same time independent speed and have the same
 21 space gaps, i.e., this synchronized flow is homogeneous in time and space. This fundamental hypothesis assumes that
 22 the driver can make an arbitrary choice in the space gap to the preceding vehicle within a finite range of space gaps at
 23 a given speed in the steady states of synchronized flow.



24 **Fig. A.1.** Fundamental hypothesis of three-phase traffic theory: (a) Qualitative representation of free flow states (F) and 2D steady states
 25 of synchronized flow (dashed region S) on a multi-lane road in the flow-density plane. (b) A part of the 2D steady states of synchronized
 26 flow shown in (a) in the space-gap-speed plane (dashed region S) (Kerner, 2009).
 27
 28

29 A.3. Phase transitions

30 In three-phase traffic theory, traffic breakdown is a phase transition from free flow to synchronized flow (F→S
 31 transition). Wide moving jams can occur spontaneously in synchronized flow only (S→J transition), i.e. due to a
 32 sequence F→S→J transitions. In real traffic, a fluctuation, whose amplitude exceeds the critical amplitude, occurring
 33 in the vicinity of the bottlenecks in the free traffic flow, will lead to the transition from free flow to synchronized flow

1 (F→S transition). Jams emerge in the synchronized flow, i.e. narrow moving jams, who spontaneously emerge in the
2 synchronized flow, move and grow in the upstream direction. Finally, these narrow moving jams (or a part of them)
3 transform into wide moving jams (S→J transition).

4 F→S transition: if before traffic breakdown occurs at a bottleneck, there is free flow at the bottleneck as well as
5 upstream and downstream in a neighborhood of the bottleneck, then the F→S transition is called as spontaneous F→S
6 transition. On the other hand, if the F→S transition is induced by the propagation of a spatiotemporal congested traffic
7 pattern, then the F→S transition is called as the induced F→S transition.

8 S→J transition: In empirical observations, S→J transition developments is associated with a pinch effect, which
9 is the spontaneous emergence of growing narrow moving jams in the synchronized flow occurring within the
10 associated pinch region of synchronized flow. If the growth of a nucleus required for moving jam emergence that
11 appearing within the synchronized flow, the S→J transition is called as the spontaneous S→J transition. Just like the F
12 →S transition, there also exists the induced S→J transition.

14 *A.4. Patterns at bottlenecks*

15 Empirical observations show that there are two main types of congested patterns at an isolated bottleneck:

16 The General Patterns (GPs): After the synchronized flow occurs upstream of the bottleneck, the wide moving
17 jams continuously emerge in that synchronized flow and propagate upstream, and then this congested pattern is often
18 called as the General Patterns (GP). However, if the wide moving jams discontinuous emerge on the road, there will
19 just have one or few wide moving jams appearing in that synchronized flow, then this congested pattern is often called
20 as the dissolving General Patterns (DGP).

21 The Synchronized Patterns (SPs): If there only exist synchronized flow upstream of the bottleneck, no wide
22 moving jams emerge in the synchronized flow, and then this congested pattern is often called as the Synchronized
23 Patterns. And as a result of the F→S transition, various synchronized flow patterns can occurs at the bottleneck, such
24 as the widening synchronized pattern (WSP), local synchronized pattern (LSP), moving synchronized pattern (MSP),
25 and alternating synchronized pattern (ASP).

27 *A.5. Models based on the three-phase traffic theory*

28 In 2002, Kerner and Klenov (2002) proposed the KK car following model, which is able to show all known
29 microscopic and macroscopic features of traffic breakdown, synchronized flow and congested patterns for the first
30 time. Later, the one-lane KKW CA model and two-lane KKS CA model (Kerner et al., 2002, 2011) are proposed. The
31 main idea of above models is the speed adaptation effect within the synchronized distance. The vehicle tends to adjust
32 its speed to the preceding vehicle as long as it is safe. Lee et al. (2004) developed the CA model mainly considered
33 mechanical restriction versus human overreaction. This model could exhibit some features of SPs and GPs. The
34 brake-light CA model (Knospe et al., 2000) and its variants (comfortable driving models) (Jiang and Wu, 2003, 2005;
35 Tian et al., 2009) have considered the brake-light effect, i.e., the simulated drivers adopt a more defensive driving
36 strategy if the braking lights of the preceding vehicle are on, i.e., if this vehicle decelerates. The comfortable driving
37 models are based on the brake-light model. They improve the latter such that their simulation results show SPs and
38 GPs as well as the diagram of congested patterns at an on-ramp bottleneck postulated in the three-phase traffic theory.
39 The CA model by Gao et al. (2007, 2009) mainly assumes that randomization depends on velocity difference. It is
40 pointed out that this model is equivalent to a combination of the KKW model and the NS model. The car following
41 model proposed by Davis (2004) incorporates the reaction delay into the optimal car following model, which can
42 describe the F→S transition. The car following model by Kerner and Klenov (2006) considered different time delays
43 on driver acceleration associated with driver behavior in various local driving situations, which can show

1 spatiotemporal congested patterns that are adequate with empirical results.

2 In order to emphasize the significance of the two-dimensional steady states of synchronized flow, Kerner and
3 Klenov (2006) proposed the speed adaption three-phase traffic models (SAMs) in the framework of fundamental
4 diagram approach. The basic hypothesis of SAMs is the double Z-characteristic for the sequence of phase transitions
5 from free flow to synchronized flow to wide moving jams ($F \rightarrow S \rightarrow J$ transitions). Based on this hypothesis, SAMs can
6 reproduce both the traffic breakdown and the emergence of wide moving jams in synchronized flow as found in
7 empirical observations. However, SAMs are not able to reproduce the local synchronized patterns (LSPs) consistent
8 with empirical results as well as some of empirical features of synchronized flow between wide moving jams within
9 general patterns (GPs). Kerner et al. attribute these drawbacks of SAMs to the lacking of the two-dimensional steady
10 states of synchronized flow.

12 References:

- 13 Ahmed, K.I., 1999. Modeling drivers' acceleration and lane changing behavior. Ph.D. thesis, Massachusetts Institute of Technology.
- 14 Bando, M., Hasebe, K., Nakayama, A., Shibata, A., Sugiyama, Y., 1995. Dynamical model of traffic congestion and numerical
15 simulation. *Physical Review E* 51, 1035-1042.
- 16 Bham, G.H., Benekohal, R.F., 2004. A high fidelity traffic simulation model based on cellular automata and car-following concepts.
17 *Transportation Research Part C: Emerging Technologies* 12(1), 1-32.
- 18 Brockfeld, E., Kühne, R.D., Wagner, P., 2005. Calibration and validation of microscopic models of traffic flow. *Transportation
19 Research Record: Journal of the Transportation Research Board* 1934(1), 179-187.
- 20 Chowdhury, D., Santen, L., Schadschneider, A., 2000. Statistical physics of vehicular traffic and some related systems. *Physics
21 Reports* 329(4), 199-329.
- 22 Davis, L., 2004. Effect of adaptive cruise control systems on traffic flow. *Physical Review E* 69(6), 066110.
- 23 Gao, K., Jiang, R., Hu, S.-X., Wang, B.-H., Wu, Q.-S., 2007. Cellular-automaton model with velocity adaptation in the framework
24 of Kerner's three-phase traffic theory. *Physical Review E* 76(2), 026105.
- 25 Gao, K., Jiang, R., Wang, B.-H., Wu, Q.-S., 2009. Discontinuous transition from free flow to synchronized flow induced by
26 short-range interaction between vehicles in a three-phase traffic flow model. *Physica A: Statistical Mechanics and its
27 Applications* 388(15), 3233-3243.
- 28 Gipps, P.G., 1981. A behavioural car-following model for computer simulation. *Transportation Research Part B: Methodological
29* 15(2), 105-111.
- 30 Greenshields, B.D., Bibbins, J., Channing, W., Miller, H., 1935. A study of traffic capacity, Highway research board proceedings.
- 31 Haight, F.A., 1963. *Mathematical Theories of Traffic Flow*. Academic Press, New York.
- 32 Helbing, D., 2001. Traffic and related self-driven many-particle systems. *Reviews of modern physics* 73(4), 1067.
- 33 Herman, R., Montroll, E.W., Potts, R.B., Rothery, R.W., 1959. Traffic dynamics: analysis of stability in car following. *Operations
34 research* 7(1), 86-106.
- 35 Jia, B., Gao, Z.-y., Ke-ping, L., Li, X.-g., 2007. *Models and Simulations of Traffic System Based on the Theory of Cellular
36 Automaton*. Science, Beijing.
- 37 Jiang, R., Wu, Q.-S., 2003. Cellular automata models for synchronized traffic flow. *Journal of Physics A: Mathematical and
38 General* 36(2), 381.
- 39 Jiang, R., Wu, Q., 2005. First order phase transition from free flow to synchronized flow in a cellular automata model. *The
40 European Physical Journal B-Condensed Matter and Complex Systems* 46(4), 581-584.
- 41 Kerner, B.S., 2004. *The physics of traffic: empirical freeway pattern features, engineering applications, and theory*. Springer Verlag.
- 42 Kerner, B.S., 2009. *Introduction to modern traffic flow theory and control: the long road to three-phase traffic theory*. Springer.
- 43 Kerner, B.S., 2012. Complexity of spatiotemporal traffic phenomena in flow of identical drivers: Explanation based on fundamental
44 hypothesis of three-phase theory. *Physical Review E* 85(3), 036110.
- 45 Kerner, B.S., Klenov, S.L., 2002. A microscopic model for phase transitions in traffic flow. *Journal of Physics A: Mathematical and
46 General* 35(3), L31.
- 47 Kerner, B.S., Klenov, S.L., 2003. Microscopic theory of spatial-temporal congested traffic patterns at highway bottlenecks. *Physical
48 Review E* 68(3), 036130.
- 49 Kerner, B.S., Klenov, S.L., 2006. Deterministic microscopic three-phase traffic flow models. *Journal of Physics A: mathematical
50 and general* 39(8), 1775.
- 51 Kerner, B.S., Klenov, S.L., Schreckenberg, M., 2011. Simple cellular automaton model for traffic breakdown, highway capacity,

1 and synchronized flow. *Physical Review E* 84(4), 046110.

2 Kerner, B.S., Klenov, S.L., Wolf, D.E., 2002. Cellular automata approach to three-phase traffic theory. *Journal of Physics A:*
3 *Mathematical and General* 35(47), 9971.

4 Knospe, W., Santen, L., Schadschneider, A., Schreckenberg, M., 2000. Towards a realistic microscopic description of highway
5 traffic. *Journal of Physics A: Mathematical and general* 33(48), L477.

6 Lee, H.K., Barlovic, R., Schreckenberg, M., Kim, D., 2004. Mechanical restriction versus human overreaction triggering congested
7 traffic states. *Physical review letters* 92(23), 238702.

8 Leutzbach, W., 1987. Introduction to the theory of traffic flow.

9 Lighthill, M.J., Whitham, G.B., 1955. On kinematic waves. II. A theory of traffic flow on long crowded roads. *Proceedings of the*
10 *Royal Society of London. Series A. Mathematical and Physical Sciences* 229(1178), 317-345.

11 Nagatani, T., 2002. The physics of traffic jams. *Reports on progress in physics* 65(9), 1331.

12 Nagel, K., Schreckenberg, M., 1992. A cellular automaton model for freeway traffic. *Journal de Physique I* 2(12), 2221-2229.

13 Neubert, L., Santen, L., Schadschneider, A., Schreckenberg, M., 1999. Single-vehicle data of highway traffic: A statistical analysis.
14 *Physical Review E* 60(6), 6480.

15 Newell, G.F., 2002. A simplified car-following theory: a lower order model. *Transportation Research Part B: Methodological* 36(3),
16 195-205.

17 NGSIM, 2006. Next generation simulation. <<http://ngsim.fhwa.dot.gov/>>.

18 Payne, H.J., 1979. FREFLO: A macroscopic simulation model of freeway traffic. *Transportation Research Record*(722).

19 Rehborn, H., Klenov, S.L., Palmer, J., 2011. An empirical study of common traffic congestion features based on traffic data
20 measured in the USA, the UK, and Germany. *Physica A: Statistical Mechanics and its Applications* 390(23), 4466-4485.

21 Richards, P.I., 1956. Shock waves on the highway. *Operations research* 4(1), 42-51.

22 Tang, T.-Q., Huang, H.-J., Gao, Z.-Y., 2005. Stability of the car-following model on two lanes. *Physical Review E* 72(6), 066124.

23 Tian, J.-f., Jia, B., Li, X.-g., Jiang, R., Zhao, X.-m., Gao, Z.-y., 2009. Synchronized traffic flow simulating with cellular automata
24 model. *Physica A: Statistical Mechanics and its Applications* 388(23), 4827-4837.

25 Tian, J.-f., Yuan, Z.-z., Jia, B., Fan, H.-q., Wang, T., 2012a. Cellular automaton model in the fundamental diagram approach
26 reproducing the synchronized outflow of wide moving jams. *Physics Letters A*.

27 Tian, J.-f., Yuan, Z.-z., Treiber, M., Jia, B., Zhang, W.-y., 2012b. Cellular automaton model within the fundamental-diagram
28 approach reproducing some findings of the three-phase theory. *Physica A: Statistical Mechanics and its Applications* 391(11),
29 3129-3139.

30 Treiber, M., Hennecke, A., Helbing, D., 2000. Congested traffic states in empirical observations and microscopic simulations.
31 *Physical Review E* 62(2), 1805.

32 Treiber, M., Kesting, A., 2013. *Traffic Flow Dynamics*. Springer.

33 Treiber, M., Kesting, A., Helbing, D., 2010. Three-phase traffic theory and two-phase models with a fundamental diagram in the
34 light of empirical stylized facts. *Transportation Research Part B: Methodological* 44(8), 983-1000.

35 Wagner, P., 2012. Analyzing fluctuations in car-following. *Transportation Research Part B: Methodological* 46(10), 1384-1392.

36 Whitham, G.B., 2011. *Linear and nonlinear waves*. Wiley-interscience.